EASR

Engineering and Applied Science Research

https://www.tci-thaijo.org/index.php/easr/index

Published by the Faculty of Engineering, Khon Kaen University, Thailand

Elastic and ultrasonic properties of fermium monopnictides

Jyoti Bala*[1)] and Devraj Singh[2)]

[1)]University School of Information, Communication & Technology, Guru Gobind Singh Indraprastha University, New Delhi 110078, India
[2)]Department of Physics, Prof. Rajendra Singh (Rajju Bhaiya) Institute of Physical Sciences for Study & Research, Veer Bahadur Singh Purvanchal University, Jaunpur-222003, U. P., India

Received 13 September 2019
Revised 26 November 2019
Accepted 3 December 2019

Abstract

Determinations of higher order elastic constants, thermal properties, mechanical properties and ultrasonic behavior have been done for fermium monopnictides. Initially, the lattice and non-linearity parameters were used to compute the higher order elastic constants at temperatures of 0K, 100K, 200K and 300K by means of the Born potential mode. Variation of Cauchy's relations has been found at higher temperature due to weak atomic interactions. The second order elastic constants (SOECs) were used to estimate mechanical parameters such as the Young's modulus, bulk modulus, Pugh's ratio, shear modulus, Zener's anisotropy factor, hardness, and Poisson ratio. On the basis of the values of these parameters, we found a brittle nature of fermium monopnictides. Furthermore, the SOECs were applied to compute the wave velocities for shear and longitudinal modes of propagation along <100>, <110> and <111> crystallographic orientations. Properties such as the lattice thermal conductivity, acoustic coupling constant, thermal relaxation time and attenuation of ultrasonic waves due to thermo-elastic and phonon-phonon interaction mechanisms have been calculated at room temperature. The results of present investigation have been analysed with available findings on other rare-earth materials.

Keywords: Fermium monopnictides, Higher order elastic constant, Thermal conduction, Ultrasonic attenuation

1. Introduction

Ultrasonics is an important branch of acoustics, which have tremendous applications in medical science [1], engineering [2] and materials science [3]. Actinide monopnictides have gained more research interest due to the presence of their partially filled electrons. Much research has been done to explain the role of f electrons in actinide monopnictides. We have found a variety of theoretical studies on Th, Np, U and Pu monopnictides/monochalcogenides that explain their mechanical and thermophysical properties with temperature and pressure in the available literature [4-11]. These studies considered their bulk moduli and phase transition properties at high pressures. Also they examined lattice dynamic properties, which are further used to evaluate specific heat of the compounds. The electronic and elastic parameters of fermium monopnictides were study with first principles calculations by Amine Monir et al. [10].These first principles computations with discussion of the phase-structure and magnetic phase as well as the magnetic and electronic properties of the FmP were presented by Bahnes et al. [11]. In these studies, the authors did not consider the temperature dependent ultrasonic attenuation for fermium monopnictides (FmP, FmAs and FmSb). So we extended the thermosphysical and ultrasonic studies on FmPn to fill this gap in the literature.

In the present investigation, we compute the second and third order elastic constants (SOECs and TOECs) of fermium monopnictides and ultrasonic velocity, Debye temperature, Debye average velocity, the acoustical coupling constant and attenuation loss due to thermoelastic relaxation and phonon viscosity phenomena along <100>, <110> and <111> orientations. The computational results are compared with other types of materials having a similar nature.

2. Theory

A theoretical approach for the computation of elastic constants and other thermo-physical properties was done to compute the temperature dependent SOECs and TOECs and ultrasonic properties along the <100>, <110> and <111> directions. It has been divided into six parts, which follow below.

2.1 Higher order elastic constants

For a crystal structure, the theory of elasticity [12-13] describes the relationship of stress and strain as

$$Y = (I + \varepsilon)X \quad (1)$$

*Corresponding author.
Email address: jyoti_pu@yahoo.com
doi: 10.14456/easr.2020.20

where Y is the deformed lattice under the application of a strain matrix ε to the initial lattice vectors X (where X is a3 x 3 unit matrix). Transformation from a unstrained domain X (x_1, x_2, x_3) into a deformed domain Y (y_1, y_2, y_3) is characterized by a Jacobian matrix J asfollows:

$$J_{ij} = \frac{\partial Y_i}{\partial X_i} \tag{2}$$

The strain parameters are taken in the Lagrangian εij [14] as:

$$\varepsilon_{ij} = \frac{1}{2}\sum_{n==1}^{3}\left(\frac{\partial y^2{}_n}{\partial x_i \partial x_j}\delta_{ij}\right) \tag{3}$$

where δ_{ij} is the Kronecker delta [15].

Since deformation is symmetric, for our convenience, we use the index notation as: (11) → 1, (22) → 2, (33) → 3, (23) → 4, (13) → 5, (12) → 6. Thus, a 3 x 3 symmetric strain matrixε, can be simplified to a 6-dimensional vector η:

$$\varepsilon = \begin{pmatrix} \varepsilon_{11} & \varepsilon_{12} & \varepsilon_{13} \\ \varepsilon_{21} & \varepsilon_{22} & \varepsilon_{23} \\ \varepsilon_{31} & \varepsilon_{32} & \varepsilon_{33} \end{pmatrix} = \begin{pmatrix} \eta_1 & \frac{1}{2}\eta_6 & \frac{1}{2}\eta_5 \\ \frac{1}{2}\eta_6 & \eta_2 & \frac{1}{2}\eta_4 \\ \frac{1}{2}\eta_5 & \frac{1}{2}\eta_4 & \eta_3 \end{pmatrix} \eta = \begin{pmatrix} \eta_1 \\ \eta_2 \\ \eta_3 \\ \eta_4 \\ \eta_5 \\ \eta_6 \end{pmatrix} =$$

$$\begin{pmatrix} \varepsilon_{11} \\ \varepsilon_{12} \\ \varepsilon_{33} \\ \varepsilon_{23} + \varepsilon_{32} \\ \varepsilon_{13} + \varepsilon_{31} \\ \varepsilon_{12} + \varepsilon_{21} \end{pmatrix} = \begin{pmatrix} \varepsilon_{11} \\ \varepsilon_{12} \\ \varepsilon_{33} \\ 2\varepsilon_{23} \\ 2\varepsilon_{13} \\ 2\varepsilon_{12} \end{pmatrix} \tag{4}$$

The elastic constants [14,16] for a B1 structured material aredefinedas:

$$C_{ijkl..} = \left(\frac{\partial^n F}{\partial \eta_{ij}\, \partial \eta_{kl}\, \partial \eta_{mn} \ldots.}\right)_{\eta=0} \tag{5}$$

where F is the free energy denisty and η_{ij}arethe components of the Langrangian strain tensor. The Voigt notation $C_{ijkl..}$ usually converts into tensor notation as (11) → 1, (22) → 2, (33) → 3, (23) → 4, (13) → 5, (12) → 6. Thus, in a cubic crystal, there will be three second order and sixthird order elastic constants. Free energy, F, can be written for the second and third ordersas:

$$F_2 = (1/2!) C_{ijkl}\, \partial \eta_{ij}\, \partial \eta_{kl} \tag{6}$$

where

$$C_{ijkl}\, \partial \eta_{ij}\, \partial \eta_{kl} =$$

$$(\eta_1, \eta_2, \eta_3, \eta_4, \eta_5, \eta_6) \begin{pmatrix} C_{11} & C_{12} & C_{12} & 0 & 0 & 0 \\ C_{12} & C_{11} & C_{12} & 0 & 0 & 0 \\ C_{12} & C_{12} & C_{11} & 0 & 0 & 0 \\ 0 & 0 & 0 & C_{44} & 0 & 0 \\ 0 & 0 & 0 & 0 & C_{44} & 0 \\ 0 & 0 & 0 & 0 & 0 & C_{44} \end{pmatrix} \begin{matrix} \eta_1 \\ \eta_2 \\ \eta_3 \\ \eta_4 \\ \eta_5 \\ \eta_6 \end{matrix}$$

$$= C_{11}(\eta_1{}^2 + \eta_2{}^2 + \eta_3{}^2) + C_{44}(\eta_4{}^2 + \eta_5{}^2 + \eta_6{}^2) + 2C_{12}(\eta_1\eta_2 + \eta_3\eta_2 + \eta_3\eta_1)$$

Similarly,

$$F_3 = (1/3!) C_{ijklmn}\, \partial \eta_{ij}\, \partial \eta_{kl}\, \partial \eta_{mn} \tag{7}$$

At a finite temperature T, the total free energy density is:

$$F^{total} = F^0 + F^{vib} \tag{8}$$

The vibrational free energy is:

$$F^{vib} = \frac{k_B T}{NV}\sum_{i==1}^{S} \ln 2 \sinh(\hbar\omega / 2 k_B T) \tag{9}$$

where V is the volume of an elementary cell, s is the number of ions in the cell, N is the number of cells in the crystal and k_B is the Boltzmann constant.F_0 is the internal energy of a unit volume of the crystal with all ions at rest at their lattice points.

Elastic constants with respect to temperature are obtained by static elastic constants plus elastic constants due to vibrational energy contribution [17-18] as follows:

$$\begin{aligned} C_{IJ} &= C_{IJ}^0 + C_{IJ}^{Vib} \\ C_{IJK} &= C_{IJK}^0 + C_{IJK}^{Vib} \end{aligned} \tag{10}$$

0 (zero) and *Vib* represent the values of the higher order elastic constants (HOECs) at 0 K and at a given temperature, respectively. Also, first term in the 7th equation is the strain derivate of F^0 and the second term is the strain derivate of F^{vib}

Energy F^0 can be expressed as:

$$F^0 = (½\ V) \sum' \emptyset_{ab}(r_0) \tag{11}$$

where r_0 is the distance between the a[th] and b[th] ion in a unit cell, $\emptyset_{ab}$is the interaction potential between ions, which is the summation of ϕ_{r0}^B= Born-Mayer potential and ϕ_{r0}^C= the Coulomb potential. Their values are given as:

$$\phi_{r0}^B = A \exp\left(\frac{-r_0}{b}\right) \text{and } \phi_{r0}^C = \pm\frac{q^2}{r_0} \tag{12}$$

where *b* is the hardness parameter or Born's repulsive parameter, q is the electronic charge, and *A* is the strength parameter. The expression to compute *A* is given as:

$$A = -3b\frac{q^2}{r_0} S_3^{(1)} \frac{1}{6\exp(-\rho_0) + 12\sqrt{2}\exp(-\sqrt{2}\rho_0)} \tag{13}$$

where $S_3^{(1)}$is the lattice sum [14] and its value is -0.58252 and $\rho_0 = \frac{r_0}{b}$

In this work, SOECs and TOECs of fermium monopnictides (FmPn) were computed at 0 K, 100 K, 200 K and 300 K using the Born model [17-18] upto the second nearest neighbour following Brugger's definition, which includes a potential model approach. The SOECs and TOECs at room temperature have been evaluated using methods developed by Mori & Hiki [18], Leibfried & Haln [19], Leibfried & Ludwig [20] and Ghate [21] for NaCl-type crystals such as the chosen fermium monopnictides FmP, FmAs and FmSb. The detailed formulae to calculate the SOECs and TOECs have been previouslypublished [22].

2.2 Mechanical constants

SOECs havebeen used to determine the values of mechanical constants [23-24] such ashardness (*Hv*), bulk modulus(*B*), shear or rigidity moduli (μ), Young's modulus(*Y*), Pugh's indicator (B/μ) and Zener anisotropy

factor (Z_A) for FmP, FmAs and FmSb. We can determine the values of the above mentioned parameters from the following equations:

$$B = \frac{C_{11}+2C_{12}}{3};\quad \mu = \mu_R + \mu_V$$

$$\text{Where } \mu_R = \frac{2.5(C_{11}-C_{12})C_{44}}{4C_{44}+3(C_{11}-C_{12})} \text{ and } \mu_V = \frac{C_{11}-C_{12}+3C_{44}}{10};$$

$$Y = \frac{9\mu B}{\mu+3B}; \upsilon = \frac{3B-2\mu}{6B+2\mu}; Hv = \frac{(1-2\upsilon)Y}{6(1+\upsilon)} \text{ and } Z_A = \frac{2C_{44}}{C_{11}-C_{12}} \quad (14)$$

2.3 Pressure derivatives and Breazeale's nonlinearity parameter

When hydrostatic pressure is applied to a cubic crystal, the arrangement of part of thespecific structure is preserved. The nonlinear elastic properties are thus defined using the concept of effective elastic constants, $C_{ij}(P)$ and is a function of pressure as:

$$C_{ij}(P) = C_{ij} + \frac{dCij(P)}{dP}P \quad (15)$$

The values of the partial derivatives of $C_{ij}(P)$ are computed using SOECs that have previous been published [25].

When the ultrasonic waves propagate through a solid material, it produces a waveform distortion thatis characteristicofthe microstructural properties of the material. The various interaction processes of these acoustic waves can be used to distinguish the harmonic generation of material. Harmonic generation arises due to the nonlinearity of the behavior of the material component, which is expressed by a nonlinear stress–strain relationship. In order to quantify the degree of nonlinearity in parameter β,it is expressed in terms of HOECs. It characterizes the simple harmonic generation of longitudinal waves given by the negative ratio of the non-linear term, transforming it to alinear term in the nonlinear wave given by [26]:

$$\beta = -(3K_2 + K_3)/K_2 \quad (16)$$

where K_2 and K_3 explained in literature [25]

2.4 Average ultrasonic velocity and Debye temperature

The materials chosen in our case for computational study are types of rock-salt. The Debye average velocity of ultrasonic wave plays a vital role in the computation of specific heat and Debye temperature of the solid material. It depends on the different modes of ultrasonic velocities. In a crystalline medium, there are three types of ultrasonic velocities (V_L, V_{S1} and V_{S2}). The ultrasonic velocities in the various crystallographic directions have been computed using the approach suggested by Thurston and Brugger [27] and expression of ultrasonic waves is discussed in the literature [28]. The expression for average ultrasonic velocity (V_D) $\theta_D$is given as:

$$\text{Along the<100>and<111>directions:} V_D = \left[\frac{1}{3}\left\{\frac{1}{V_L^3}+\frac{2}{V_s^3}\right\}\right]^{-\frac{1}{3}} \quad (17)$$

$$\text{Along the <110> direction:} V_D = \left[\frac{1}{3}\left\{\frac{1}{V_L^3}+\frac{1}{V_{s1}^3}+\frac{1}{V_{s2}^3}\right\}\right]^{-\frac{1}{3}} \quad (18)$$

The Debye temperature plays a very important role characterizing a solid. It relates the elastic and thermos-physical properties of a material. The expression to evaluate the Debye temperature is:

$$\theta_D = \frac{h}{k_B}\left(\frac{3n}{4\pi}\frac{N\rho}{M}\right)^{\frac{1}{3}} V_D \quad (19)$$

where n=atomic number in a unit cell, N=Avogadro's constant,ρ=density, h=Planck's constant, k_B=Boltzmann's constant, M=molecular weight.

2.5 Thermal conductivity

Thermal conductivity depends on the anharmonicity of the inter-atomic potential. It is an important parameter in various applications. For example, low thermal conductivity materials are used as thermal barrier coatings (e.g., for gas turbines). Thermal conductivity is associated with the transfer of energy in a material through lattice vibration. Under this consideration and using the Cahill approach [29], the thermal conductivity along three modes of lattice vibration are given as:

$$\kappa = \frac{k_B}{2.48} \times n^{\frac{2}{3}}(V_L + V_{S1} + V_{S2}) \quad (20)$$

2.6 Ultrasonic attenuation

When ultrasonic waves propagate through a specimen, their energy is dissipated in various form such as absorption, diffraction, and scattering, among others. The main cause of attenuation of ultrasonic waves arises due to phonon-phonon interaction (p-p), thermo-elastic relaxation and electron-phonon (e-p) interaction mechanisms [30].

At high temperatures, the attenuation of ultrasonic waves occurs by two mechanisms, i.e., by the thermo-elastic phenomenon and p-p interactions. The e-p mechanism is absent at high temperatures (≥100 K) because there is no interaction taking place between electrons and acoustical phonons. In our study, we calculated attenuation/loss of ultrasonic waves propagating along various orientations in fermium monopnictides at room temperature. Attenuation per frequency squared of ultrasonic waves is due to the phonon-phonon interaction mechanism in the longitudinal mode $\left(\frac{\alpha}{f^2}\right)_L$ and, shear modes of propagation$\left(\frac{\alpha}{f^2}\right)_s$ are given as:

$$\left(\frac{\alpha}{f^2}\right)_L = \frac{4\pi^2\tau_l E_0 D_L}{6\rho V_L^3}, \left(\frac{\alpha}{f^2}\right)_{S_1} = \frac{4\pi^2\tau_s E_0 D_{S1}}{6\rho V_{S_1}^3}$$

$$\text{and } \left(\frac{\alpha}{f^2}\right)_{S_2} = \frac{4\pi^2\tau_s E_0 D_{S2}}{6\rho V_{S_2}^3} \quad (21)$$

Here E_0=Energy density at given temperature, f=frequency of ultrasonic wave, D=acoustic coupling constant and τ= thermal relaxation time. E_0 was computed using the θ_D/T table of the AIP Handbook [31].

Table 1 Temperature dependencies SOECs and TOECs of FmP, FmAs and FmSb [in 10^{11} N/m^2]

Material	Temp.[K]	C_{11}	C_{12}	C_{44}	C_{111}	C_{112}	C_{123}	C_{144}	C_{166}	C_{456}
FmP	0	5.35	1.53	1.57	-86.60	-6.21	2.45	2.61	-6.40	2.59
FmP[10] B1	0	18.85	1.26	4.61	-	-	-	-	-	-
	100	5.41	1.48	1.57	-86.70	-6.04	2.12	2.62	-6.38	2.59
	200	5.58	1.39	1.57	-87.47	-5.69	1.62	2.64	-6.38	2.59
	300	5.77	1.30	1.57	-88.46	-5.34	1.11	2.66	-6.38	2.59
FmAs	0	4.95	1.32	1.36	-82.15	-5.34	2.16	2.27	-5.47	2.26
FmAs [10] B2	0	15.02	1.46	5.52	-	-	-	-	-	-
	100	5.03	1.26	1.35	-82.42	-5.12	1.77	2.28	-5.46	2.26
	200	5.21	1.18	1.35	-83.34	-4.77	1.27	2.29	-5.46	2.26
	300	5.41	1.09	1.34	-84.37	-4.42	0.76	2.31	-5.46	2.26
FmSb	0	4.29	0.99	1.00	-74.37	-3.94	1.65	1.73	-4.04	1.73
FmSb [10] B2	0	10.09	3.34	5.17	-	-	-	-	-	-
	100	4.39	0.92	1.00	-74.73	-3.70	1.23	1.74	-4.03	1.73
	200	4.57	0.85	1.01	-75.68	-3.36	0.72	1.76	-4.03	1.73
	300	4.75	0.76	1.01	-76.71	-3.01	0.19	1.77	-4.03	1.732

Table 2 First order pressure derivate FOPD (in 10^{-12} N/m^2) and β of FmP, FmAs and FmSb at room temperature

Materials		FmP	FmAs	FmSb
dC_{11}/dp		10.140	10.558	11.428
dC_{12}/dp		1.987	1.925	1.805
dC_{44}/dp		0.0200	0.0400	0.1556
β	<100>	12.319	12.595	13.159
	<110>	5.858	5.871	5.913
	<111>	1.500	1.529	1.605

Thermal phonons are distorted when ultrasonic waves pass through a medium. The time in which it regains its original shape through a relaxation mechanism is termed, relaxation time, and is defined as:

$$2\tau_{th}C_V V_D^2 = 2\tau_{sh}C_V V_D^2 = \tau_{long}C_V V_D^2 = 6\kappa \quad (22)$$

The specific heat over a unit volume (C_V) also has been computed using data from the AIP Handbook [31]. The acoustic coupling constant is a scaling parameter for the interchange of acoustic energy into thermal energy in the relaxation process or vice versa. Itis given as:

$$D = 9\langle(\gamma_i^j)^2\rangle - \frac{3\langle\gamma_i^j\rangle^2 C_V T}{E_\theta} \quad (23)$$

The ultrasonic attenuation caused by thermo-elastic relaxation is expressed as [30]:

$$\left(\frac{\alpha}{f^2}\right)_{th} = \frac{4\pi^2 < \gamma_i^j >^2 \kappa T}{2\rho V_L^5} \quad (24)$$

3. Results and discussion

3.1 Second and third order elastic constants

SOECs and TOECs are evaluated over a temperature range 0-300 K with the help of a lattice parameter for fermium monopnictides FmPn (Pn=P, As and Sb) that have diameters of 5.57 Å,5.76 Å, 6.17 Å, respectively. The hardness/non-linearity parameter b is 0.303 Å for all the chosen materials. The obtained values of the SOECs and TOECs are given in Table 1. The elastic constants such as C_{11}, C_{166} and C_{144}increased, while C_{12}, C_{112} and C_{123} decreased with the temperature, while C_{456} was constant at all the temperatures.

The changes in the elastic constants were due to the change in atomic interactions with temperature. If inter-atomic distance changed with temperature, then interaction potential also changed, which altered elastic values. The calculated values of the third-order elastic constants were found sensitive to external stresses of temperature and small changes, except C_{111}. The high value of C_{111} shows crystal anisotropy. The values of C_{11}, C_{12} and C_{44}were compared with the first principles calculations of Monir *et al*. [10] for FmP. The comparison results have variations due to the different approaches used to compute the elastic constants. Similar trends were found in other FCC materials with same range of elastic constants at higher orders such as strontium chalcogenides [32] curium monopnictides [33] and actinide monocarbides [34].

3.2 Mechanical properties

The obtained SOECs were applied to evaluate the first order pressure derivative FOPD values of elastic constants as well as the mechanical properties at room as presented in Tables 2 and 3. We also evaluated the nonlinearity parameter β of the ultrasonic wave of fermium monopnctides along three different directions. From the analysis of Table 2, we surmise that the highest values are obtained for the FmSb along the <100> axis. We observe small linear growth with atomic weight having the same rate of variation. This implies that the waveform distortion is slower for fermium monopncitdes. The first order pressure derivatives, dC_{11}/dp, dC_{12}/dp, are negative for all fermium compounds. dC_{44}/dp is negative whereas FmP can be positive or negative depending on the crystal type. Also, dC_{111}/dp increases with molecular weight whereas the values of dC_{12}/dp, dC_{44}/dp decrease with increased molecular weight of the chosen materials. This is due to the effect of the elastic constants of materials. The obtained FOPD values and β were compared with praseodymium monopnictides [25].

Table 3 B, Y, μ, B/μ, Z_A, *Hv* andρ of FmP, FmAs and FmSb at room temperature

Fermium Monopnictides	*B* (10^{10}Nm^{-2})	*Y* (10^{10}Nm^{-2})	μ (10^{10}Nm^{-2})	*B*/μ	Z_A	*Hv* (10^{10}Nm^{-2})	ρ (g/cm^3)
FmP	2.793	4.468	1.811	1.54	0.703	0.322	11.057
FmP [10]	7.12		5.99	1.18	0.787		
FmAs	2.529	4.027	1.631	1.56	0.626	0.288	11.488
FmAs [10]	6.76						
FmSb	2.093	3.291	1.329	1.57	0.507	0.232	10.731
FmSb [10]	4.86						

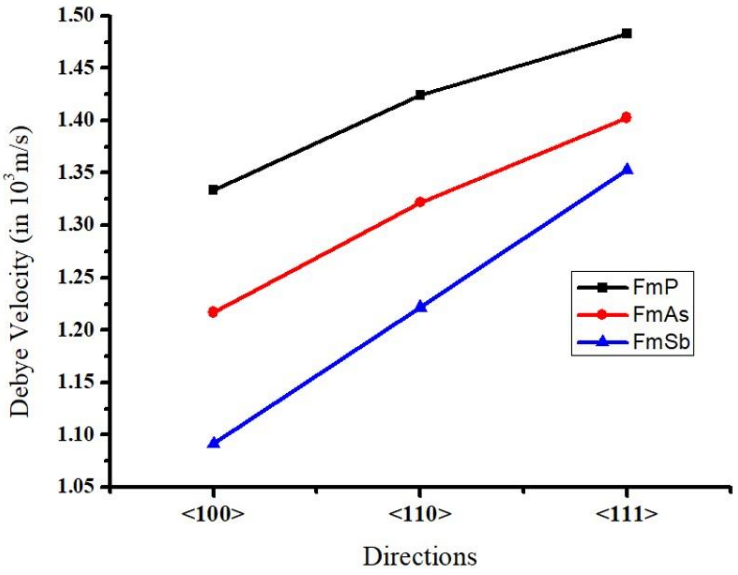

Figure 1 Directional dependency of V_D for FmPn at room temperature

The values of mechanical constants such as the bulk (*B*), Young's (*Y*)and shear moduli (μ), as well as Pugh's indicator (B/μ),the Zener anisotropy factor (Z_A), and hardness (*Hv*) were computed and presented in Table 3.

From this table, we observed that there is a deviation in the value of the bulk modulus calculated by Amine Monir et al. [10] using first principles investigation since we used a different theoretical approach. Computational values of bulk and shear moduli for fermium monopnictides at room temperature satisfied the Born mechanical stability criterion $(B = \frac{C_{11}+2C_{12}}{3} > 0, C_s = \frac{C_{11}-C_{12}}{2} > 0, C_{44} > 0)$. Hence, our method of computation for SOECs and TOECs is consistent. The Pugh indicator *B*/μ [35] has been found between 1.54 and 1.57, so these compounds exhibit brittle behaviour at room temperature. It is clear from Table 3 that FmP has the largest value of μ (18.11GPa) among all the monopnictides compounds, whereas the lowest shear modulus (13.29 GPa) for FmSb, shows that this monopnictide has little resistance to deformation. FmP has the largest Young's modulus (44.68 GPa) compared to other compounds. This shows that FmP is the stiffest among these monopnictides. Compressibility of a material is inversely related to its bulk modulus. With increased temperature, the C_{11} factor of the elastic constant increased, which in turn increased the value of the bulk modulus, and hence compressibility decreased with increased temperature. The C_{12} factor of the elastic constant decreased with increased temperature, which shows that the anisotropy of the material decreased with increased temperature. The densities of fermium monopnictides Fm, P, As and Sb are 9.7 gcm^{-3}, 1.82 gcm^{-3}, 5.78 gcm^{-3}and 6.68 gcm^{-3} respectively. The densities of FmP, FmAs and FmSb, in our case, are 11.06 gcm^{-3}, 11.49 gcm^{-3} and 10.73 gcm^{-3} respectively. This indicates that materials became lighter after alloying with fermium.

3.3 Directionally dependent thermal and ultrasonic properties

The values of ultrasonic average velocity/Debye velocity and Debye temperature (θ_D) for fermium monopnictides along three different orientations are calculated using SOECs and are shown in Figures 1-2, respectively. Due to the unavailability of experimental data for fermium monopnicitides, we relate the results with other FCC based materials such as semimetallic materials [34]. It was found that the Debye velocity and Debye temperature follow the same trend similar as semimetallics compounds. The Debye velocity along various crystallographic directions is depicted in Figure 1. The Debye temperature is shown in Figure 2, also along various orientations. The lattice atomic weight of phosphorous is less than other fermium monopnictides since FmP has highest Debye velocity and Debye temperature along the<111> crystallographic axis, as shown in Figures 1-2. The Debye temperature is an important parameter that can be used to calculate ultrasonic attenuation/losses along three different orientations and is presented in Table 4. The evaluated values of thermal conductivity are visualized in Figure 3. FmP has the highest thermal conductivity along the <111> direction at room temperature as is presented in Figure 3. Hence, the FmP material is the most thermally conductive material.

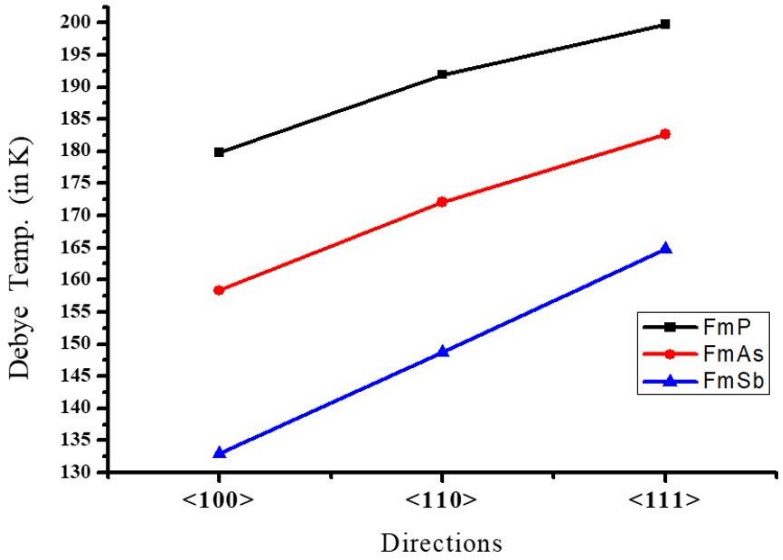

Figure 2 Directionally dependent θ_D for FmPn at room temperature

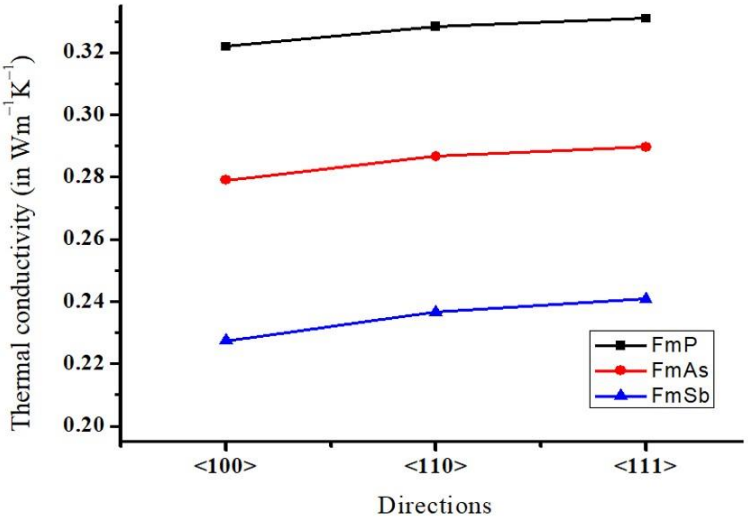

Figure 3 Directionally dependent thermal conductivity

Table 4 Directionally dependent κ (in $Wm^{-1}K^{-1}$), D_L, D_S, τ_{th} (in ps), $(\alpha/f^2)_{th}$, $(\alpha/f^2)_l$, $(\alpha/f^2)_s$ and $(\alpha/f^2)_{total}$ all (α/f^2) in $10^{-13}Nps^2m^{-1}$ at room temperature

Fermium Monopnictides	Direction	κ	D_L	D_{s1}	τ_{th}	$(\alpha/f^2)_{th}$	$(\alpha/f^2)_L$	$(\alpha/f^2)s$	$(\alpha/f^2)_{total}$
FmP	<100>	0.3219	14.53	1.053	5.7	0.0048	1.903	0.484	2.391
	<110>	0.3283	17.00	0.931	5.1	0.0187	2.357	0.337	2.713
	<111>	0.3309	15.03	18.21	4.8	0.0174	2.065	4.738	6.820
FmAs	<100>	0.2789	15.18	1.062	6.6	0.0052	2.382	0.668	3.055
	<110>	0.2866	17.76	0.891	5.8	0.0223	3.059	0.482	3.563
	<111>	0.2897	15.36	19.20	5.2	0.0224	2.560	5.555	8.137
FmSb	<100>	0.2274	16.55	1.088	8.1	0.0053	3.186	1.070	4.261
	<110>	0.2366	19.47	0.832	6.8	0.0267	4.325	0.668	5.019
	<111>	0.2409	16.09	21.27	5.6	0.0312	3.336	6.550	9.917

From Table 4, we also observed that values of the acoustic coupling constants (D_L, D_S) are much less for FmP monopnictide compounds. FmAs and FmSb correspond to different orientations at room temperature. On inspection of Table 4, it can be seen that the magnitude of the thermal relaxation time is on the order of 10^{-11} s, which confirms its semi-metallic nature [36-37] that increases with the lattice molecular weight of monopnictides. Also, the value of ultrasonic attenuation is lowest for FmP along the<100>direction, so FmP has potential applications in industry. The order and nature of ultrasonic attenuation/loss is found similar to other rare-earth materials such as;

gadolinium monopnictides [38], ytterbium monopnictides [39], rare-earth monoarsenides [40] and scandium based intermetallics [41].

4. Conclusions

A simple theoretical approach was used to evaluate the ultrasonic properties of fermium monopnictides. It is found in good agreement with the results available for other rare-earth monopnictides. At room temperature, FmP has the largest value of its higher order elastic constant, 5.774 GPa. Thus, the elastic properties of FmP are greater than those of FmAs and FmSb. The Born-stability criterion was followed by these actinide monopnictides and thus these materials are mechanically stable. The hardness of the materials decreased with increasing molecular weight of fermium monopnictides. The Pugh's indictor is found to be less than 1.75, indicating that fermium monopnictides are brittle in nature. The ultrasonic average velocity supports anisotropic characterization for these monopnictides. Also, FmP has the highest value of average ultrasonic velocity (along the<100> direction at room temperature). Thus, FmP is the most appropriate material for crystallographic study at room temperature. Its Debye temperature and the thermal conductivity were found highest for FmP along the <111> crystallographic axis. So, FmP(the lightest material) has good thermal performance. The quantum of the thermal relaxation time for these materials is of the order of picoseconds, which confirms the semi-metallic behaviour of fermium monopnictides at room temperature. The value of total thermal attenuation is minimal for FmP and maximal for FmSb. The value of ultrasonic attenuation was found lowest for FmP along the<100> direction, where the shear wave was polarised along the <110> direction and highest along the <111> direction. Minimal attenuation of the ultrasonic wave when passed through a material along the <100> direction reveals that this is most suitable direction for an anisotropic study of these materials. Hence, the achieved results deliver a good understanding of the elastic and thermophysical properties of the chosen fermium monopnictides, which may be used for further research investigations and in material producing industries.

5. References

[1] Kaatze U. Non-critical fluctuations of liquids: Cinderella of ultrasonic spectroscopy?. Int J Thermophys. 2014;35:1976-89.

[2] Tripathi S, Agarwal R, Vashisth R, Singh D. Deflection analysis of capacitive micromachined ultrasonic transducer with InP nanowires. 7th International Conference on Signal Processing and Integrated Networks (SPIN); 2020 Feb 27-28; Noida, India. USA: IEEE; 2020. p. 355-8.

[3] Vargaftik NB, Kozhevnikov VF, Gordeenko AM, Arnold DI, Naurzakov SP. Experimental study of the ultrasonic velocity in liquid cesium at high temperatures and pressures. Int J Thermophys. 1986;7:821-8.

[4] Gerward L, Olsen JS, Benedict U, Luo H, Itié JP, Vogt O. Bulk moduli and high-pressure phases of ThX compounds: I. the thorium monopnictides. High Temp High Press. 1988;20:545-52.

[5] Gerward L, Staun Olsen J, Benedict U, Dabos S, Vogt O. Bulk moduli and high-pressure phases of the uranium rocksalt structure compounds-I. The monochalcogenides. High Pres Res. 1989;1(4):235-51.

[6] Olsen SJ, Gerward L, Benedict U, Dabos S, Vogt. O. Bulk moduli and high-pressure phases of the uranium rocksalt structure compounds: II. the monopnictides. High Pres Res. 1989;1(4):253-66.

[7] Dabos S, Dufour C, Benedict U, Spirlet JC, Pagès M. High-pressure x-ray diffraction on neptunium compounds: recent results for NpAs. Physica B+C. 1986;144(1):79-83.

[8] Dabos-Seignon S, Benedict U, Heathman S, Spirlet JC, Pages M. Phase transformation of AnX compounds under high pressure (An ≡ Np, Pu; X ≡ Sb, Te).J Less Common Met.1990;160(1):35-52.

[9] Gensini M, Gering E, Heathman S, Benedict U, Spirlet JC. High-pressure phases of plutonium monoselenide studied by X-ray diffraction. High Pres Res. 1990;2(5-6):347-59.

[10] Amine Monir ME, Ullah H, Baltach H, Mouchaal Y. First-principles investigations on the structural, elastic, phase stability and electronic properties of the binary monopnictide compounds based on the fermium FmX (X = P, As, and Sb). Comput Condens Matter. 2017;13:131-8.

[11] Bahnes A, Amine Monir ME, Baltach H, Mouchaal Y, Kenane A, Bekhti-Siad A. Half-metallic ferromagnetism in V-doped FmP binary monopnictide compounds: an ab initio calculations. J Supercond Nov Magn. 2019;32(3):705-14.

[12] Murnaghan FD. Finite deformation of an elastic solid. New York: Dover publications; 1967.

[13] Pham HH, Cagin T. Lattice dynamics and second and third order elastic constants of iron at elevated pressure. CMC-Comput Mater Con. 2010;16(2):175-94.

[14] Wallace DC. Thermodynamics of crystlas. New York: Wiley; 1972.

[15] Mehl MJ, Osburn JE, Papacontantopoules DA, Klein BM. Sturctural properties of orders liquid high melting temperature intermetallic alloys from 1st principles total energy calculations. Phy Rev B. 1990;41:10311-23.

[16] Brugger K. Thermodynamic definition of higher order elastic coefficients. Phys Rev. 1964;133:A1611-2.

[17] Born M, Mayer JE. Zur Gittertheorie der Lonenk-ristalle. Z Phys. 1932;75:1-18.

[18] Mori S, Hiki Y. Calculation of the third- and fourth-order elastic constants of alkali halide crystals. J Phys Soc Jpn. 1978;45:1449-56.

[19] Leibfried G, Hahn H. Zur Temperaturabhängigkeit der elastischen Konstanten von Alkalihalogenidkristallen. Z Phys. 1958;150:497-525.

[20] Leibfried G, Ludwig W. Theory of anharmonic effect in crystal. Solid State Phys. 1961;12:275-444.

[21] Ghate PB. Third-order elastic constants of alkali halide crystals. Phys Rev. 1965;139:A1666-74.

[22] Bhalla V, Singh D, Jain SK. Mechanical and thermophysical properties of cerium monopnictides. Int J Thermophys. 2016;37(3):1-17.

[23] Singh D, Tripathy C, Paikaray R, Mathur A, Wadhwa S. Behaviour of ultrasonic properties on SnAs, InTe and PbSb. Eng Appl Sci Res. 2019;46(2):98-105.

[24] Singh D, Bhalla V, Bala J, Wadhwa S. Ultrasonic investigations on polonides of Ba, Ca, and Pb. Z Naturforsch A. 2017;72(11):977-83.

[25] Bhalla V, Kumar R, Tripathy C, Singh D. Mechanical and thermal properties of praseodymium monopnictides: an ultrasonic study. Int J Mod Phys B. 2013;27(22):1-28.

[26] Bains JA, Breazeale MA. Third order elastic constants and Gruinesium paramters of silicon and germanium between 300 and 3^0K. Phys Rev B.1976;13:3623.
[27] Thurston RN, Brugger K. Third-order elastic constants and the velocity of small amplitude elastic waves in homogeneously stressed media. Phys Rev. 1964; 133:A1604-10.
[28] Tripathi S, Agarwal R, Singh D. Nonlinear elastic, ultrasonic and thermophysical properties of lead telluride. Int J Thermophys. 2019;40:78.
[29] Cahill DG, Watson SK, Pohl RO. Lower limit to the thermal conductivity of disordered crystals. Phys Rev B. 1992;46:6131-40.
[30] Mason WP. Physical Acoustics. Vol. III B. New York: Academic Press; 1965.
[31] Gray DE. American Institute of Physics Handbook. New York: McGraw Hill; 1981.
[32] Varshney D, Jain S, Shreya S, Khenata R. High-pressure and temperature-induced structural, elastic and thermodynamically properties of strontium chalcogenides. J Theor Appl Phys. 2016;10:163-93.
[33] Tripathy C, Singh D, Paikaray R. Behaviour of elastic and ultrasonic properties of curium monopnictides. Can J Phys. 2018;96(5):513-8.
[34] Singh D, Kumar A, Bhalla V, Thakur RK. Mechanical and thermophysical properties of actinide monocarbides. Mod Phys Lett B. 2018;32(21):1-9.
[35] Pugh SF. XCII. Relations between the elastic moduli and the plastic properties of polycrystalline pure metals. Philos Mag. 1954;45:823-43.
[36] Kor SK, Pandey G, Singh D. Ultrasonic attenuation in semi-metallie GdX single crystals (X= P, As, Sb and Bi) in the temperature range 10 to 300K. Indian J Pure Appl Phys. 2001;39:510-3.
[37] Singh D, Pandey DK, Singh DK, Yadav RR. Propagation of ultrasonic waves in neptunium monochalcogenides. Appl Acoust. 2011;72(10):737-41.
[38] Singh D, Tripathi S, Pandey DK, Gupta AK, Singh DK, Kumar J. Ultrasonic wave propagation in semi-metallic single crystals. Mod Phys Lett B. 2011;25(31):2377-90.
[39] Pandey DK, Singh D, Bhalla V, Tripathi S. Temperature dependent elastic and ultrasonic properties of ytterbium monopnictides. Ind. J. Pure Appl. Phys. 2014;52:330-6.
[40] Bhalla V, Singh D, Jain SK, Kumar R. Ultrasonic attenuation in rare-earth monoarsenides. Pramana- J Phys. 2016;86:1355-67.
[41] Bala J, Singh D, Pandey DK, Yadav CP. Mechanical and thermophysical properties of ScM (M: Ru, Rh, Pd, Ag) intermetallics. Int J Thermophys. 2020;41:1-13.